Available online at www.sciencedirect.com
SCIENCE DIRECT®
Nuclear Instruments and Methods in Physics Research A 497 (2003) 60–74
NUCLEAR INSTRUMENTS & METHODS IN PHYSICS RESEARCH Section A
www.elsevier.com/locate/nima

Detector design issues for compact nuclear emission cameras dedicated to breast imaging

Craig S. Levin*

San Diego VA Medical Center, Nuclear Medicine Division, and UCSD School of Medicine, Department of Radiology, 3350 La Jolla Village Drive, San Diego, CA 92161, USA

Abstract

Certain gamma ray and positron emitting radiotracers have shown great promise for use in the detection, diagnosis and staging of breast cancer. Unfortunately, standard nuclear emission cameras (SPECT, PET) found in the clinic are not practical for breast imaging of these emissions due to inadequate spatial and energy resolutions and sensitivity, large and awkward size, and relatively high cost per study. High spatial and energy resolutions and sensitivity are needed for good lesion detectability. Due to these limitations of standard cameras, there has been recent research into the development of small, compact nuclear emission imagers dedicated for close-proximity breast imaging. The small detector head size means a variety of exotic detectors or collimators may be implemented to improve spatial and energy resolution and sensitivity performances at a reasonable cost. In this paper, we will present some of the compact gamma ray and annihilation photon imaging detector designs that have been proposed and/or developed for dedicated breast imaging. We will review the physics and discuss the advantages and disadvantages of various detector configurations. Finally we will estimate the fundamental spatial resolution potential available with close-proximity nuclear emission imaging and discuss how one may approach those limits through proper detector design.
Published by Elsevier Science B.V.

Keywords: Breast imaging; Nuclear medicine; Position-sensitive detectors; Detectors; Functional imaging

1. Introduction: motivation for the small camera concept

Radiolabeled molecular imaging provides in vivo functional information about the biochemistry and/or molecular biology of processes of interest. This technique is often used in imaging cancer, due to highly specific signatures for malignancy. In particular, certain gamma ray [e.g. ^{99m}Tc-Sestamibi (MIBI)] and positron emitting [e.g. ^{18}F-fluorodeoxyglucose (FDG)] radiotracers have shown great promise for use in the detection, diagnosis and staging of breast cancer. Unfortunately standard nuclear emission cameras [Single Photon Emission Computed Tomography (SPECT), Positron Emission Tomography (PET)] found in the clinic are not practical for breast imaging of these emissions due to their inadequate spatial and energy resolutions and sensitivity, large and awkward size, and relatively high cost per study. The large and awkward detector head of a standard gamma camera cannot in general be brought very close to the breast, accepts background activity from other organs, and allows only certain views to be taken. These factors result in

*Tel.: +1-858-552-7511.
E-mail address: clevin@ucsd.edu (C.S. Levin).

0168-9002/03/$ - see front matter Published by Elsevier Science B.V.
PII: S0168-9002(02)01893-4

non-optimal spatial resolution, lower image contrast, and limited usefulness in breast imaging. Sensitivity of standard gamma ray collimators is also not optimized for breast imaging. The large detector separation and relatively coarse detector elements of a standard PET system means limited sensitivity and spatial resolution for breast imaging. In addition, the cost-effective PET detector design employed in commercial systems has low resolution, leading to reduced image contrast. Thus, there are limited breast lesion detection capabilities for standard nuclear emission cameras. Finally, the relatively high cost per study using standard nuclear imaging systems limits their practicality for clinical breast imaging.

Due to these limitations of standard cameras, there has been recent research into the development of small, compact nuclear emission imagers dedicated for breast imaging. A compact gamma ray camera is essentially a miniaturization of the standard gamma camera. The most common design used for a compact positron annihilation photon imager is two small flat detector heads operating in electronic coincidence. A compact imager has the advantages of ease of use, flexibility, and accuracy of positioning at multiple orientations. The detector head(s) can be brought in contact with the breast for close-proximity imaging, which allows optimal spatial resolution for both gamma ray and coincident annihilation photon imaging. The close-proximity also significantly increases the sensitivity for the annihilation photon application and certain gamma ray collimator designs. The compact design facilitates detector head positioning at orientations that reduce or eliminate the background activity from other organs, such as the heart, that often accumulate a significant portion of the tracer. A compact imager is portable and could be brought into the mammography suite to assist the radiologist in cancer detection, diagnosis or staging. If highly compact, the unit can be incorporated into a mammography unit to image the breast while under compression for improved lesion detectability, and in registration with the mammogram, for combined structural and functional information. A small, relatively low cost device could also contribute to lowering the cost per study, which may allow nuclear imaging of the breast to become more practical from a clinical perspective.

The small detector head also means a variety of exotic detectors or collimators may be implemented to improve spatial and energy resolution and sensitivity performances at a reasonable cost. In this paper, we will present some of the compact gamma ray and annihilation photon imaging detector designs that have been proposed and/or developed for dedicated breast imaging. We will review the physics and discuss the advantages and disadvantages of various detector configurations. Finally we will estimate the best spatial resolutions available with close-proximity nuclear emission imaging and discuss how one may approach those limits through proper detector design.

2. Lesion detectability factors for single- and coincident annihilation photon imaging

Detector design effects lesion detection capabilities. Lesion detectability factors may be assessed using tumor phantoms where one may vary the lesion size and depth, tumor:tissue activity concentration ratio, acquisition time (statistics), and background activity. We performed previous studies of such issues with a high resolution, high sensitivity, small gamma ray camera performing close-proximity imaging [1]. It was determined that, assuming adequate accumulation of ^{99m}Tc and 5–10 min of imaging, the three most significant factors determining lesion detectability were the size and depth of the lesion, and the degree of Compton scatter background present [1]. The lesion depth effects measured spatial resolution, amount of normal tissue activity in front of the lesion seen by the detector, and degree of photon attenuation. Breast compression will improve lesion detectability in planar nuclear emission breast imaging because it decreases the effective lesion depth seen by the detector(s). Higher spatial resolution imagers will help to improve identification of smaller and deeper lesions. Identification of increased biochemical activity of smaller tumors before structural changes occur could mean earlier

cancer detection. Scatter leads to positioning errors, which means images with a superimposed background haze and loss of lesion to background contrast. Higher energy resolution systems allow the use of narrower energy windows for better rejection of Compton scatter from in and out of field-of-view (FOV) sources while at the same time maintaining good sensitivity. Fig. 1 demonstrates these issues of improved lesion identification with larger lesions and tighter energy discrimination for a small NaI(Tl)-position-sensitive PMT (PSPMT) camera [1,2]. The relatively good intrinsic point source energy resolution of that system of $\sim$12% FWHM at 140 keV [1], allows adequate sensitivity to be maintained for narrower energy window data. Fig. 2 shows example energy spectra measured with this small NaI(Tl)-PSPMT camera for a ^{99m}Tc point source, a breast tumor phantom consisting of a set of hot spheres of different sizes with a cold background, and the same hot spheres with a warm background. In the right plot of Fig. 2 we see the significant presence of background activity measured by this system with a 5:1 ^{99m}Tc activity concentration ratio, even though there is only a 140 cm^3 volume of background activity present. Comparing the middle and right figures of Fig. 2, we see that much of the measured activity within the photopeak in the right figure comes from the background rather than tumor activity within the FOV that enters the camera without scatter. This fraction of accepted background to tumor activity increases for deeper tumors.

With $\geqslant$5:1 uptake ratio, a 5 mm diameter tumor 3 cm deep into tissue could be identified with such a single-photon camera within 5-10 min [1]. Would one be able to improve upon these capabilities with a coincident annihilation photon imager?

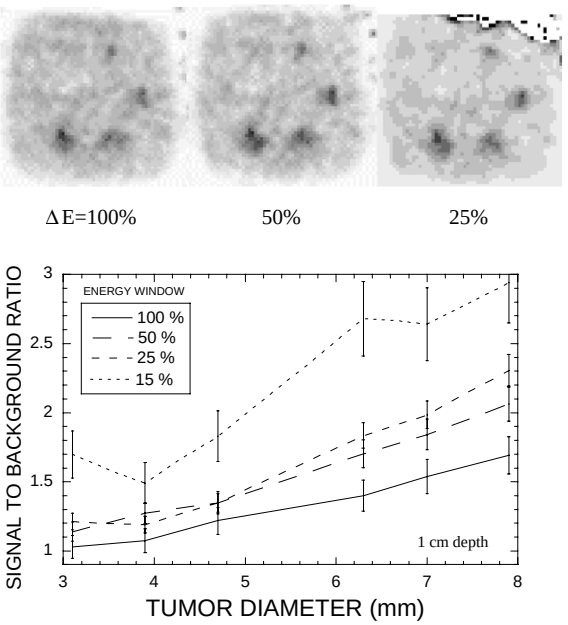

Fig. 1. Top: Images of a tumor phantom for three different energy windows with the tumors 1 cm deep into a warm background with 5:1 tumor/background ^{99m}Tc acstivity concentration ratio. Bottom: The ratio of the activity measured in an ROI surrounding the different tumors to the background (S/B) improves as the energy window is narrowed. Due to the relatively good intrinsic energy resolution of 12% FWHM at 140 keV, adequate sensitivity was maintained for narrower energy windows. Note the large increase in S/B with lesion size as well.

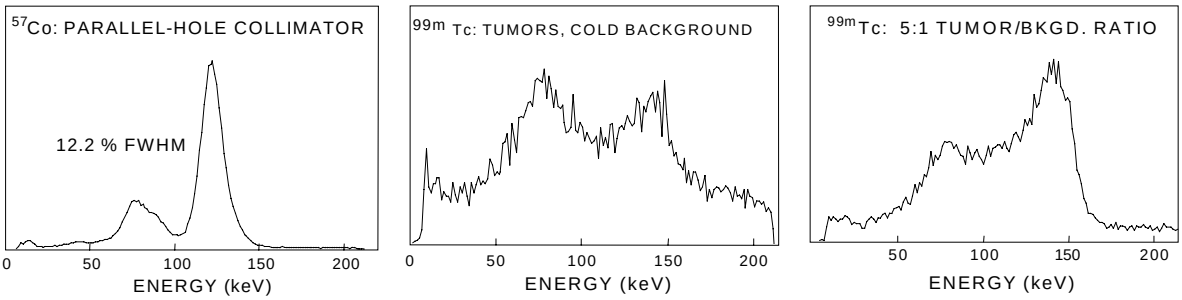

Fig. 2. Left: Point source energy spectrum. Middle: Breast phantom energy spectrum with hot tumors, cold background. Right: Breast phantom energy spectrum with hot tumors, warm background (5:1 tumor:background concentration ratio). Volume of background used: 136 cm^3.

Probably not. We expect the same three factors (lesion size and depth, and extent of Compton background) to determine lesion identification capabilities for coincident annihilation photon imagers as well. Compact single-photon imagers can be produced with comparable spatial and energy resolution to coincidence imagers, which are the most important qualities needed to address the three dominant lesion detectability limiting factors (size, depth, scatter background). In fact, although Compton scatter and overall absorption in tissue is less probable for 511 keV than for 140 keV photons, their scatter angular distribution is broader, which could possibly even worsen detectability limits. Thus, assuming $\geqslant$5:1 uptake ratio of the tracer, and close-proximity imaging with comparable spatial resolution, from the device point of view, it is expected that a single-photon imager provides comparable breast lesion detectability limits compared to a coincidence imager. This statement is supported by recent results from small single- and coincidence annihilation photon emission camera studies [1,3]. However, if the nature of the particular breast cancer under study involves significantly higher uptake ratios for a positron-labeled tracer compound (e.g. FDG) compared to the single-photon-labeled compound (e.g. MIBI), then the detectability limits may improve with coincidence imaging.

3. Position-sensitive detector design issues

3.1. Collimator designs

For annihilation photon imagers, collimation is provided electronically through coincident detection of the two annihilation photons. For single-photon imagers, a physical collimator is necessary. Eqs. (1) and (2) describe the collimator resolution (in one dimension, FWHM) and efficiency equations for the parallel- and pinhole designs [4], which are two common gamma ray collimators currently implemented in small FOV dedicated gamma ray breast imager designs.

Parallel-hole:

$$R \approx d + \frac{dx}{h - 2/\mu}$$

$$E \approx 0.068 \left(\frac{d}{h - 2/\mu}\right)^2 \left[\frac{d^2}{(d+t)^2}\right] \quad (1)$$

Pinhole:

$$R \approx \sqrt{d[d + 2\mu^{-1}\tan(\alpha/2)](h+x)/h}$$

$$E \approx d[d + 2\mu^{-1}\tan(\alpha/2)]\cos^3\theta/16x^2 \quad (2)$$

where d is the hole/aperture diameter, h the collimator thickness/height, t the septal thickness for the parallel-hole collimator, x the tumor-collimator distance, μ the linear attenuation length of the collimator material, α the apex angle of the pinhole collimator, and θ the source azimuth angle subtended at the pinhole. The total single-photon system spatial resolution is a convolution of the collimator and intrinsic detector resolution components.

As seen from Eqs. (1) and (2), gamma ray collimators show spatial resolution degradation with increasing source to collimator distance, which for close-proximity, "in-contact" breast imaging corresponds to the lesion depth. Glancing at the expressions for efficiency, one trick that can be used to improve the sensitivity for gamma ray collimators used in close-proximity breast imaging is to decrease the collimator height. Using a $\leq$2cm thick parallel-hole collimator, for example, the result is a camera that focuses only on relatively shallow lesions, perhaps $<$3 cm deep, which may be acceptable especially for imaging compressed breasts. Fig. 3 shows how the resolution of a point source 1 cm above a parallel-hole collimator improves with collimator thickness for a small single-photon camera. A 2 cm thickness allows significantly higher sensitivity compared to a standard 3–4 cm thick, low-energy-high-resolution (LEHR) parallel-hole collimator, and good spatial resolution for a close source-collimator distance. Note for close-proximity, in-contact imaging, collimator resolution does not necessarily dominate the system spatial resolution anymore, and so the detector resolution becomes an important contribution to the system spatial resolution. Note also that although the sensitivity significantly

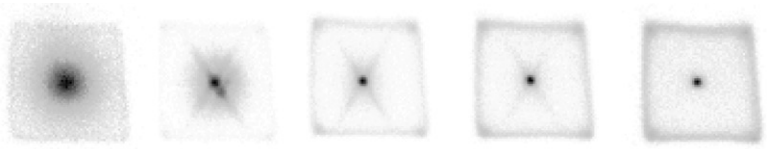

Fig. 3. Images of a ^{57}Co point source using a 6 cm FOV NaI(Tl)-PSPMT camera for different LEHR collimator thickness varying from 0 to 2.0 cm. The relative collimator sensitivities are from left to right: 1.00:0.113:0.016:0.011:0.009. The corresponding system spatial resolutions are 13.6, 5.7, 3.6, 3.3, and 3.3 mm FWHM, respectively. Relative scaling is used for display.

Table 1
Properties of common scintillation crystals used in small FOV nuclear emission imager designs

Scintillator	Effective Z	Density (g/cc)	Radiation length (mm)[a]	Relative light yield	Refractive index	Decay time (ns)	Peak emission wavelength (nm)	Hygroscopic?	Rugged?
NaI(Tl)	51	3.67	3.4	100	1.85	230	410	Yes	No
CsI(Tl)	54	4.51	2.2	135	1.79	1000	530	No	Yes
CsI(Na)	54	4.51	2.2	75	1.79	650	420	No	Yes
BGO	74.2	7.13	10.5	15	2.15	300	480	No	Yes
LSO(Ce)	65.5	7.4	11.6	75	1.82	40	420	No	Yes
GSO(Ce)	59	6.71	14.0	25	1.91	30–60	440	No	Yes

[a] Radiation lengths quoted for NaI(Tl), CsI(Tl) and CsI(Na) are for 140 keV photons; Those values quoted for BGO, LSO, and GSO are at 511 keV.

changes with source-collimator distance for the pinhole collimator, it does not for the parallel-hole design.

3.2. Detector materials for photon imaging

Table 1 lists properties of various inorganic scintillation crystals that have been used in small FOV single and coincident annihilation photon imager designs. Scintillation crystals are appealing materials for imaging because of the relatively good stopping power for high-energy photons (high Z, high density, and thick) and robust signal produced (high visible light yield, good spectral match to PMT photocathode), and relatively low cost. As a result, the majority of small nuclear emission imagers developed to date have used scintillation crystals. We will thus focus much of our discussion in this paper on position-sensitive scintillation crystal designs. Table 2 lists properties of various room-temperature semiconductor crystals that have been implemented in small FOV single-photon emission imagers. Due to the limited thickness of semiconductor detectors, their use in medical nuclear emission imaging has been almost exclusively limited to low-energy ($\leqslant$ 140 keV) imaging. However, with a significant investment, by using different array orientations or stacking many array levels together, one may be able to achieve adequate detection efficiency for 5ll keV coincidence imaging in the future.

For completeness, we mention the possibility of developing compact position-sensitive gas-filled detectors for breast imaging. Options are to use high pressure or liquid noble gases, or low-pressure gases with lead or high stopping power scintillation crystal converters [5,6]. These systems offer very high spatial resolution, and relatively low costs, but perhaps lower overall sensitivity and energy resolution, higher dead area, and less compactness compared to the scintillation crystal systems.

Table 2
Properties of common semiconductors used in small FOV emission imager designs

Semiconductor	Atomic number Z	Density ρ(g/cm^3)	Band gap E_g (eV)	Ave. e–h creation energy w (eV)	Resistivity (Ωcm)	Electron mobility μ_e(cm^2/V/s)	Hole mobility μ_h(cm^2/V/s)	Electron lifetime τ_e (s)	Hole lifetime τ_h (s)
Si	14	2.33	1.12	3.62	2.3×10^5	1500	600	3×10^{-3}	3×10^{-3}
CdTe	48–52	6.06	1.47	4.43	3.0×10^9	1000	80	10^{-6}	10^{-6}
$Cd_{.8}Zn_{.2}Te$	30–52	5.81	1.5–2.2	5.0	2.5×10^{11}	1350	120	6×10^{-7}	2.5×10^{-8}
HgI_2	80–53	6.4	2.13	4.15	10^{13}	100	4	10^{-7}	10^{-8}

All values quoted are at 300°K.

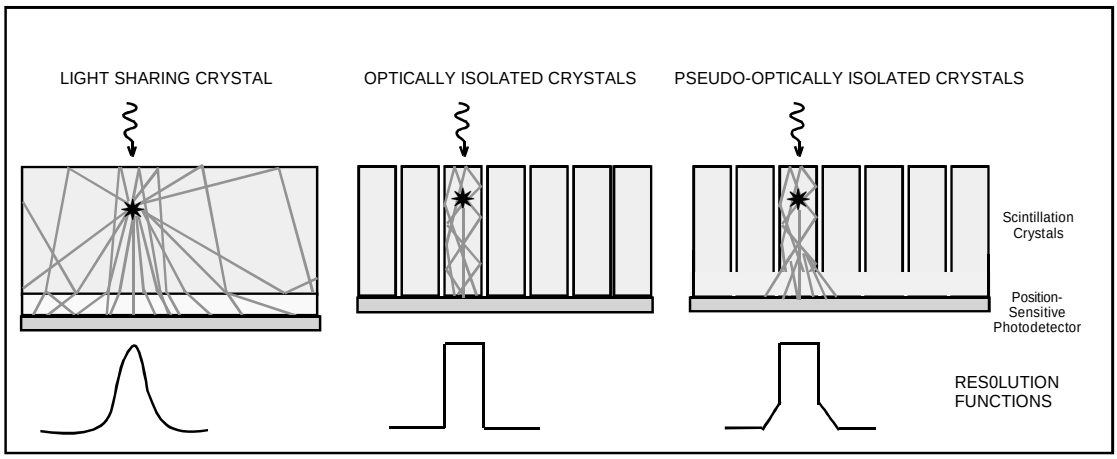

Fig. 4. Schematic depiction of basic schemes for positioning scintillation crystal light using position-sensitive photodetectors. Left: Single-crystal design—light is shared through the crystal and contiguous diffuser by several photodetectors. Middle: Discrete crystal design—light is constrained and focused onto one spot on the photodetector plane. Right: Hybrid design–crystals are not cut all the way through and light is diffused at the bottom or a separate light diffuser is used. Theoretical response functions are depicted at the bottom. Only partial FOV shown.

3.3. Position sensitive scintillation crystal configurations

Common position-sensitive scintillation crystal configurations used in single- and annihilation photon imagers are shown in Fig. 4. In the single crystal design (Fig. 4, left), light is shared among several photodetectors. A scintillation event may be positioned, for example, using an appropriate weighted mean of the signals from the various photodetectors involved. The spatial response function in this case is Gaussian-shaped. In the discrete crystal design (Fig. 4, middle), the detector comprises many optically isolated crystals and created light is constrained and focused to one spot on the photodetector plane. The spatial response function in this case is rectangular-shaped. One may also use a hybrid design (Fig. 4, right) where the crystals are not completely optically isolated and some controlled light sharing over the photodetector plane occurs. This can be achieved by either not cutting the crystals all the way through, or by adding a separate light diffuser between the crystal array and photodetector plane. The hybrid design is useful in those cases where the pitch of the photodetectors is courser than that of the discrete scintillation crystals in an array and some controlled light sharing is needed for optimal positioning of scintillation events. The latter approach is also a useful technique to reduce the

number of photodetector readout channels required.

Some advantages of the single, continuous crystal design: better light collection, higher detection sensitivity per area (no crystal dead area), better spatial uniformity (no sharp discontinuities), continuous positioning (no pixellation artifacts), for single-photon imaging standard collimators may be used, simplicity, and lower cost. Advantages of the discrete crystal design: selectable intrinsic spatial resolution dictated by crystal width, focused light (better signal–noise ratio [*S*/*N*] for a one–one crystal-photodetector design), improved spatial linearity (response is roughly the same for all crystal positions), detector scatter rejection capability (for one–one crystal-photodetector coupling). Fig. 5 demonstrates that the spatial linearity is improved for the discrete crystal array compared to the single, continuous crystal design of a small imager. This is true since the amount and shape of the light distribution projected onto the photodetector plane is similar for all crystals in a discrete-crystal array, which is not the case for a continuous crystal.

For close-proximity imaging, high intrinsic spatial resolution becomes important for optimal system spatial resolution for both the single- and coincident photon designs. Due to the selectable high intrinsic spatial resolution, the discrete crystal design (Fig. 4, middle and right) has been the most popular choice for compact emission imager designs [7–11]. The importance of high spatial resolution for lesion detection has been discussed. We focus for a moment on the issue of scintillation light collection. High light collection is important for optimal scintillation detector energy resolution and good *S*/*N*. The importance of high-energy resolution for lesion detectability has been emphasized. For ultra-high intrinsic spatial resolution and good detection efficiency the crystals should be skinny ($\leqslant$ 2 mm wide) and long. However, for such a crystal, the light collection aspect ratio is poor, and it is difficult to extract a large fraction of the available scintillation light from the crystal for each scintillation event. Fig. 6 shows the point source energy spectra measured for a collimated point source on (left) a $60 \times 60 \times 6\,\mathrm{mm}^3$ NaI(Tl) continuous crystal and (right) one individual $2 \times 2 \times 6\,\mathrm{mm}^3$ crystal from an array, coupled to a PSPMT. The continuous crystal design has significantly larger scintillation light pulses and higher resulting-energy resolution because a higher fraction of the available light is collected.

Fig. 7 depicts the major mechanism for light loss in long and narrow crystals. The fraction of the available scintillation light that is collected from the end of a crystal depends on the *aspect ratio* (ratio of the crystal length to readout

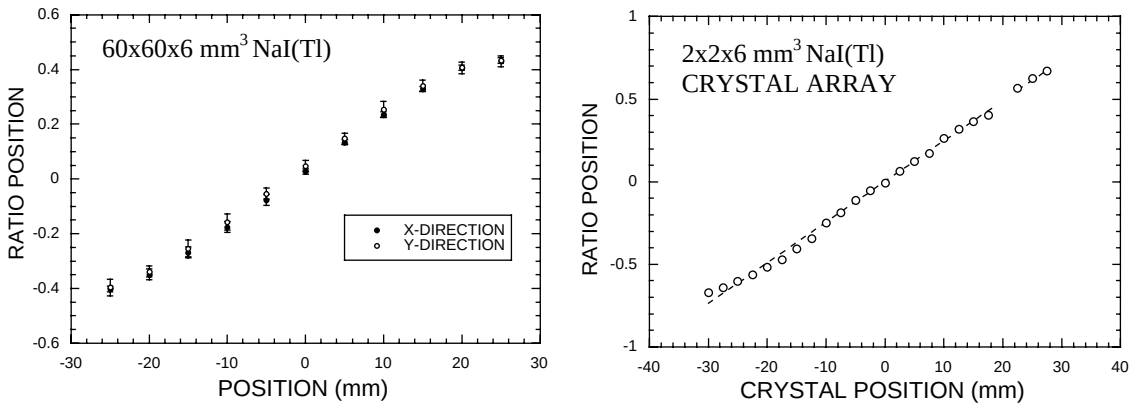

Fig. 5. Plots of the line source position measured from the resulting images as a function of its true position allows an assessment of spatial linearity for imaging with the $60 \times 60 \times 6\,\mathrm{mm}^3$ continuous crystal (left) and the segmented crystal array comprising $2 \times 2 \times 6\,\mathrm{mm}^3$ crystals (right). Spatial linearity is improved at the edges for the discrete array.

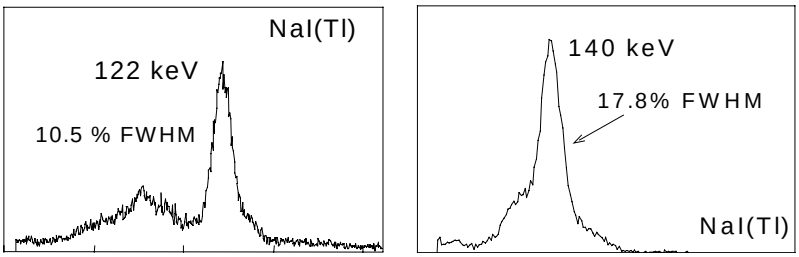

Fig. 6. Collimated point source energy resolution measured in a (left) $60 \times 60 \times 6\,\mathrm{mm}^3$ continuous crystal, and (right) $2 \times 2 \times 6\,\mathrm{mm}^3$ discrete crystal from a crystal array.

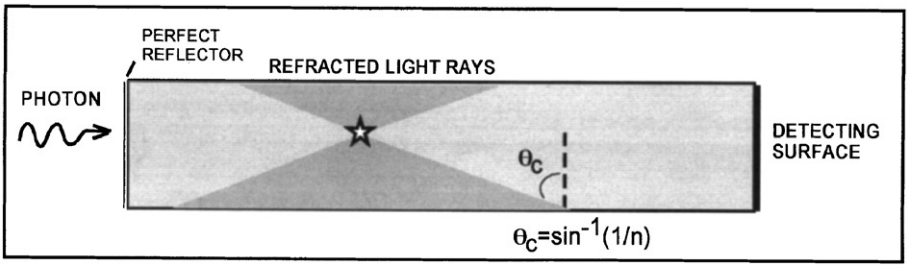

Fig. 7. Depiction of major light loss mechanism in long and skinny crystals. The poor aspect ratio means a significant fraction of the available light is lost through the crystal sides. Most of the light impinging on the crystal sides at angles less than the critical angle (shaded) will exit the crystal and not be piped down to the small detecting surface.

cross-sectional area). Other factors are the degree of light absorption and trapping within the crystal and at the surfaces. Due to a poor light collection aspect ratio, a significant amount of the light is lost at the sides of or trapped within a long and narrow crystal, and unless ideal crystal surface conditions exist that promote total internal reflection, only a small fraction of the available light will be collected. The maximum fraction of collected light may be estimated by inspection of Fig. 7 assuming ideal conditions and a crystal length much greater than its width. This fraction depends on the fraction of light rays impinging upon the crystal surface at angles less than the critical angle θ_c for that medium, which turns out to depend only upon n:

The solid angle of lost light, Ω_L, through one crystal side face is approximately:

$$\Omega_L \approx \pi \tan^2 \theta_c \approx \pi/n^2$$

where n = refractive index; θ_c = critical angle.

Thus, the maximum fraction of light collected at the end of a long and narrow crystal is roughly:

$$f \approx 1 - 1/n^2. \quad (3)$$

Fig. 8 shows the results of Monte Carlo simulations of light collection from the ends of long and narrow scintillation crystals for various crystal types used in small FOV single- and coincident photon imagers. Two different surface conditions were simulated. The ideal situation is a perfectly polished crystal with an air gap. This condition will promote internal reflection toward the end. The other surface condition is ground (diffuse, Lambertian). This second surface is typically what is available for commercially supplied, highly pixellated scintillation crystal arrays. Both surfaces had a 98% reflectivity, diffuse, Lambertian reflector applied on all surfaces except the detecting end. Even with the most ideal surface conditions, only a fraction of the light is collected. The simulation results for the most ideal case compares well with

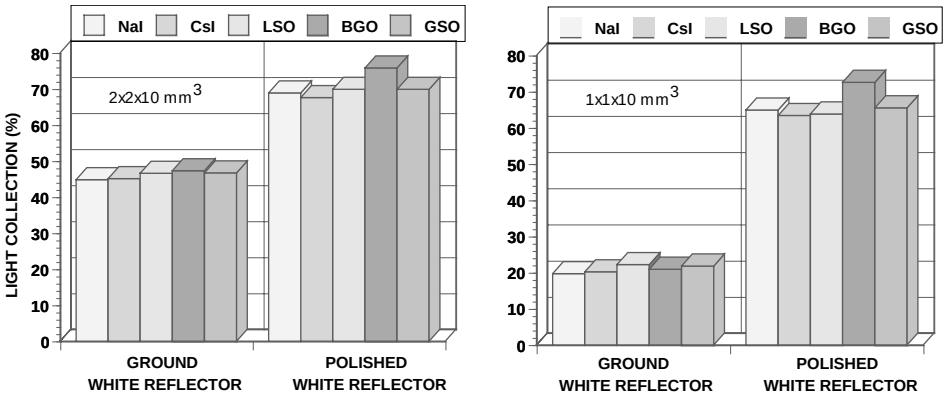

Fig. 8. Average fraction (%) of the available scintillation light collected from the ends of different length and type of scintillation crystals (1 and 2 mm wide) for two different crystal surface conditions. Even with the most ideal surface conditions, only a fraction of the light is collected. In reality, the fraction lies somewhere between that for the two surface extremes (for example, 20–60% for $1 \times 1 \times 10\,\mathrm{mm}^3$ LSO).

equation 3. In reality, the light collection fraction lies somewhere between that for the two extremes of ground and polished surfaces (for example, 20–60% for $1 \times 1 \times 10\,\mathrm{mm}^3$ LSO). For better light collection, the crystal length may be reduced, but that would mean a decrease in detection efficiency and sensitivity. The crystal width could be increased to extract more light (and also increase *S*/*N* per pixel), but that would reduce the desired spatial resolution. Such compromises are a reality in existing small FOV emission imager designs [7–11].

3.4. Position-sensitive photodetectors

The most commonly used position-sensitive photodetector in small FOV emission imagers is the position-sensitive PMT. The first small FOV cameras in recent times used the cross-wire anode, mesh dynode variety PSPMT [12]. The newer small FOV imager designs [7–9] use the metal channel dynode PSPMT variety, which has the advantage of reduced lateral charge diffusion for higher spatial resolution compared to the mesh dynode structure. The recently developed flat-panel PSPMT also uses the metal channel dynode structure, but has a larger sensitive area, higher anode packing fraction, and is flatter than the earlier models. Thus, the flat-panel design is ideal for use in small FOV breast imagers. There are a few choices for readout of PSPMT anode signals. For example, all anode signals may be read out in parallel or resistive charge division may be used to reduce the number of readout channels. For devices with a large number of anode channels, such as cross-wire anode PSPMTs, or systems comprising multiple metal channel dynode PSPMTs, configuring small groups of connected anodes may allow the best compromise between positioning precision, number of channels and detector *S*/*N* [13].

In recent years there has also been great progress in the development of semiconductor photodetector arrays. Because of limited wafer size and the stage of the technology, these developments are ideally suited to small FOV emission imagers. Three promising photodetector array technologies for small FOV imagers are the PIN photodiode (PD) [14], the avalanche photodiode (APD) [15], and the silicon drift detector (SDD) [16]. The silicon PD has the basic advantages of compactness and a factor of three times higher peak quantum efficiency for visible light compared to the bialkali PMT photocathode. One commercial vendor [17] currently manufactures a small CsI(Tl)-PD gamma camera system that has been used for close-proximity breast imaging. The APD has the advantages of higher gain (due to the

presence of a region of high electric field where avalanche occurs within the device structure), better S/N (since the surface leakage current is not amplified by the avalanche process and series noise effects are low due to the relatively high gain), and more precise timing (due to higher gain and S/N) compared to the PD. The SDD consists of a relatively large cathode, a tiny, low capacitance anode for comparable series noise contribution and S/N to that of a photodiode of comparable anode area, and electric field shaping electrodes. A main advantage of the SDD is that the relatively large cathode area per pixel means that fewer SDD elements and readout channel electronics are required to cover the same imaging area. Although traditionally these were gain = 1 devices, a very recent development [18] has made possible the concept of an avalanche SDD. Due to the relatively low gain of semiconductor photodetectors, the system noise is typically limited by the amplifier stage. This means each channel requires a low noise, charge-sensitive preamplifier. Because of the significant uncorrelated noise from each element, and low gain resistive division is typically not an option for semiconductor photodetector arrays.

Similar to that described in Section 3.3 and Fig. 4, scintillation crystals may be coupled 1–1 to matched semiconductor photodetector channels for optimal S/N ratio, with all the light focused onto one photodetector element. Or, with adequate light diffusion, a pseudo-discrete crystal array or a continuous, non-segmented scintillation crystal may be coupled to a semiconductor photodetector array.

PSPMTs have the advantages of high gain, low noise, and simplicity. Because of the high gain, system noise is not limited by the amplifier stage so special low-noise charge sensitive preamplifier electronics are not required. Semiconductor photodetectors have advantages of high quantum efficiency, high compactness, low dead area, fine sampling for higher resolution, and, after some initial development investments, potential for lower manufacturing costs. It should be noted that the flat-panel PSPMT will improve compactness of PMT designs for small FOV imagers.

3.5. High density, high z, high band gap semiconductor detector arrays

For completeness, we also mention that there has also recently been great progress in the development of high stopping power, room temperature semiconductor arrays for direct detection of high-energy photons [19]. The detectors are typically formed from a monolithic, single crystal and the position sensitivity is established by the collection electrode pixellation pattern. An ionizing event results in the creation of tens of thousands of electron–hole pairs. A relatively strong electric field is applied across the material. The holes drift toward the cathode and the electrons toward the anode. The event position is determined by which electrode pixel has the largest induced signal.

These direct detection imagers have the potential advantage of higher energy resolution, since all of the photon energy goes into forming electron–hole pairs, which go directly into forming the electronic signal. For example, in CdTe, a 140 keV photon will create roughly 32,000 electron–hole pairs which go directly into the basic formation of the signal. The same photon will create perhaps 5200 photons in a NaI(Tl) scintillation crystal of which only roughly 1000 will be converted into photoelectrons. So the basic electronic signal before amplification is 30 times larger for the semiconductor detector. However, the lower mobility holes are trapped at impurity sites, resulting in incomplete charge collection and a low-energy tailing of the energy spectrum photopeak. Another advantage of semiconductor detectors is the potential for ultra-high intrinsic spatial resolution [19]. In fact, the hole-trapping has reduced effect on signal formation for smaller pixel detectors [20]. Because no scintillation crystal is required, the direct detection semiconductor design has even higher potential for compactness. Finally, assuming more widespread use, a semiconductor technology has potential for reduced costs.

Compared to direct detection semiconductor detectors, scintillation detectors have the following advantages: higher yield of detector quality crystals; thicker detectors can be manufactured

Table 3
Promising imaging detector technologies

Position-sensitive electronic detector technology	Advantages	Drawbacks
Flat-panel PSPMT (scintillation detection)	High gain, low noise, compact, high packing fraction, charge division readout, simplicity	Low quantum efficiency, relatively expensive
PIN photodiodes (scintillation detection)	High quantum efficiency, high spatial resolution, compact	Unit gain, many pixels required, each with low noise, charge- sensitive preamplifiers
Avalanche photodiodes (scintillation detection)	High quantum efficiency, high spatial resolution, gain, compact	Difficult to manufacture, many pixels required, each with charge sensitive preamplifiers
Silicon drift detectors (or Silicon Avalanche drift detectors) (scintillation detection)	High quantum efficiency, can cover large area with fewer electronic channels, compact	Relatively low gain, requires low noise, charge sensitive preamps, relatively high leakage current
CdZnTe arrays (direct detection)	Large signal, high spatial resolution, extremely compact	Lower stopping power (thin detectors), hole trapping, many pixels required, each with low noise charge sensitive preamps

for higher detection efficiency; higher uniformity of spatial and energy response; there are no charge trapping issues; and standard collimators may be used for certain single-photon imager designs. Scintillation detectors also have higher gain and low noise per channel, and so the electronic readout is simplified for an initial lower system cost. Most of the small FOV breast imager developments to date have used scintillation detectors. Table 3 summarizes some of the advantages and drawbacks of promising detector technologies discussed in this section.

4. Spatial resolution potential for emission imaging of the breast

We have discussed how optimizing spatial resolution is important to small lesion identification, which could mean earlier breast cancer detection. This motivates the question: what is the fundamental spatial resolution potential for emission imaging of the breast and can we achieve this potential with appropriate detector design? The limitations on spatial resolution are different for single- and coincidence annihilation photon imaging. In this section we present the results of calculations of the fundamental physical limits on spatial resolution for these two modes of emission imaging.

4.1. Physical spatial resolution limits in single-photon breast imaging

For standard single-photon imaging, spatial resolution is limited by the collimator properties. Two common collimators used in small FOV imager single-photon imaging are the parallel- and pinhole designs. In Section 3, we presented the analytical expressions that describe the resolution and efficiency performance of these two collimator types. The attainable system spatial resolution is a convolution of the collimator and detector components. Spatial resolution may be optimized by a combination of close-proximity imaging and fine intrinsic detector resolution. To illustrate potentials for spatial resolution in single-photon imaging, Fig. 9 plots system spatial resolution (FWHM) as a function of intrinsic detector resolution for various source-collimator distances for the two types of collimators. Intrinsic spatial resolution can be selected by going to a discrete, pixellated detector design. For close-proximity imaging, the intrinsic detector resolution plays a larger role in the system resolution. With an intrinsic detector resolution of 1 mm, a collimator hole (aperture) size of 1.2 mm, and 2 cm tumor-collimator distance, the system resolution is roughly 2 mm FWHM for both the parallel- and pinhole designs. The corresponding geometrical efficiencies and sensitivities are 5×10^{-5} and

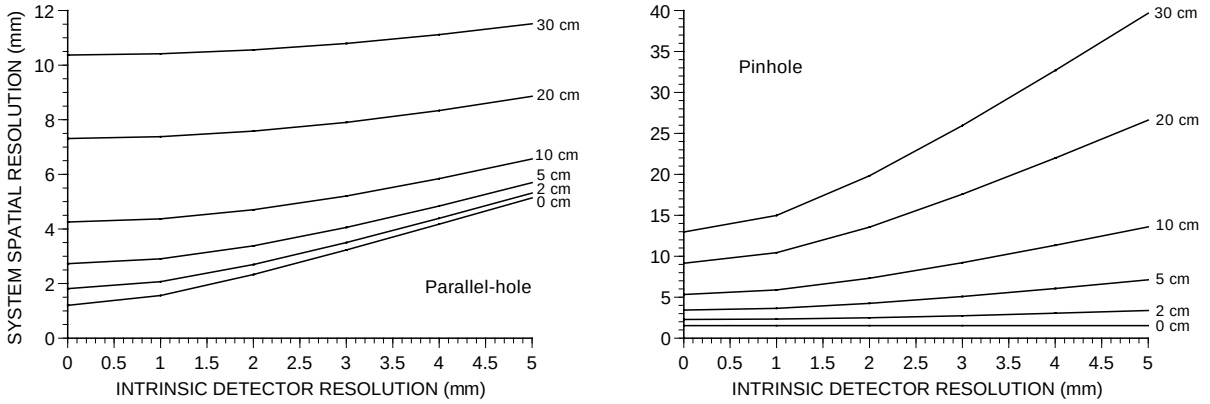

Fig. 9. Calculated spatial resolution (FWHM) as a function of intrinsic detector spatial resolution for various source-collimator distances for parallel-hole (left) and pinhole (right) collimators. We have assumed a collimator hole diameter of 1.2 mm, height of 4.0 cm, and $\mu = 27\,\mathrm{cm}^{-1}$ for lead at 140 keV. For the pinhole an apex angle of 45° and the magnification factor have been included.

2×10^{-4}, and 2.0 and 7.3 cps/μCi, respectively for the parallel- and pinhole collimators. With the stated collimator parameters used to generate the data in Fig. 9, there does not seem to be a significant advantage to go to a smaller intrinsic detector resolution than 1 mm. If one wanted to push the spatial resolution limits even more, one would have to decrease the collimator hole (aperture) size, but this would lead to significantly lower sensitivity. For example, if the hole (aperture) size were reduced to 600 μm, the system spatial resolutions would be on the order of 1 mm FWHM, but the sensitivities would decrease by an additional factor of 5 and 4 for the parallel- and pinhole designs, respectively, which may be unacceptably low for practical imaging. One possible way to gain back some of the sensitivity while maintaining high resolution might be to form a ring of multiple small FOV detectors around and in close contact with the breast.

4.2. Physical spatial resolution limitations in coincidence annihilation photon breast imaging

The three main physical factors that limit spatial resolution in coincidence annihilation photon imaging are positron range, annihilation photon non-collinearity, and intrinsic detector resolution [21]. A perhaps more accurate description of the "positron range" contribution to the spatial resolution is the fluctuation in the endpoint coordinates of the positron. Because each emitted positron is emitted in a different direction and travels a distinct finite distance before stopping, there will be a fluctuation in the precise location of the positron emission point. The three-dimensional extent of this blurring function depends on the endpoint energy of the positron emitter and the particular tissue traversed. Since the most common tracers discussed for PET breast imaging are ^{18}F-labeled we will focus on predicting spatial resolution potential using this isotope. In the following discussion, we assume breast tissue has the effective density and Z of water. Fig. 10 shows the projection onto the plane of 100 Monte Carlo simulated positron tracks in water from a point source of ^{18}F. This trajectory calculation [21] included factors such as, (1) the rate of energy loss $\mathrm{d}E/\mathrm{d}x$ of positrons from the ionization and excitation of the water molecules, (2) multiple Coulomb scatter of the positrons with the water nuclei, (3) hard positron–electron collisions that produce so called *delta electrons*, that acquire enough energy from the collision to produce their own ionization track, and (4) the form of the ^{18}F positron kinetic energy spectrum. Fig. 11 shows a one-dimensional histogram of the x-coordinates from 100,000 simulated ^{18}F positron trajectories. This cusp-like distribution will be considered as

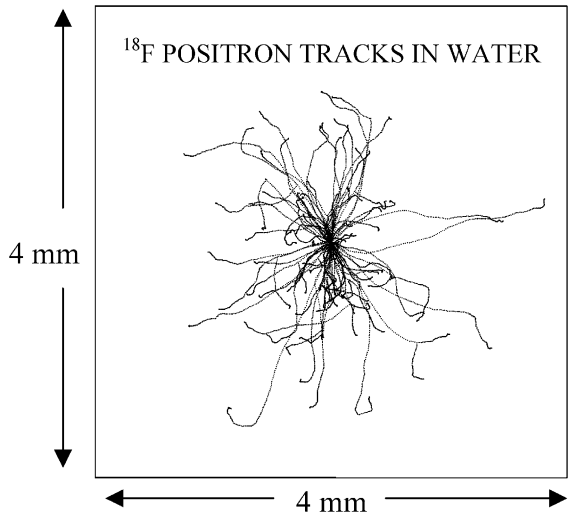

Fig. 10. Projections onto the plane of 100 Monte Carlo calculated positron trajectories from an ^{18}F point source in water. Adapted from Ref. [21].

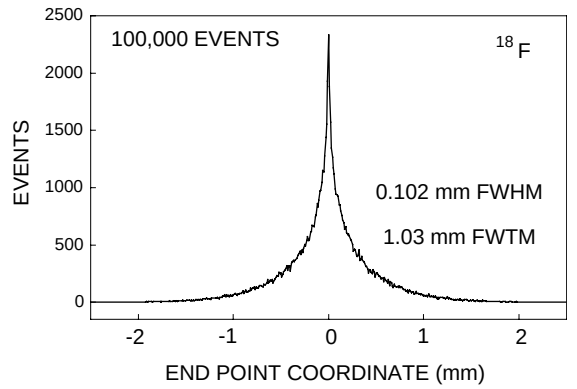

Fig. 11. Histogram of x-coordinates of 100,000 calculated positron trajectories represents the 1-D resolution blurring function for positron range. Adapted from Ref. [21].

the positron range contribution to spatial resolution blurring in one-dimension for ^{18}F.

The extent of blurring due to annihilation photon non-collinearity and detector resolution are easier to model. The annihilation photon non-collinearity effect is due to the fact that the positron and electron are not in fact always at rest when they annihilate, and in order to conserve energy and momentum, the annihilation photons will not always be emitted 180° apart. The extent of the linear fluctuations in positioning annihilation events caused by this effect will depend solely on the system geometry. Empirically it has been determined that the photon non-collinearity effect for a point source produces a 1-D blurring kernel approximately in the form of a Gaussian function with a FWHM of roughly $0.0022*D$, where D is the system detector separation or diameter in millimeters (see Ref. [21]). The detector resolution blurring is related to how precisely the detected annihilation photons may be positioned at the detectors. If the detector elements are much smaller than the system diameter, the point source coincidence detection response function in 1-D is roughly triangular in shape with a FWHM of roughly one-half the detector element width [21].

The total system resolution is a convolution of the three basic blurring kernels for positron range (cusp-like, depends on positron emitter), photon non-collinearity (Gaussian-like, depends on detector separation), and coincidence detection resolution (triangular shape, depends on detector element size). Fig. 12 plots the fundamental system

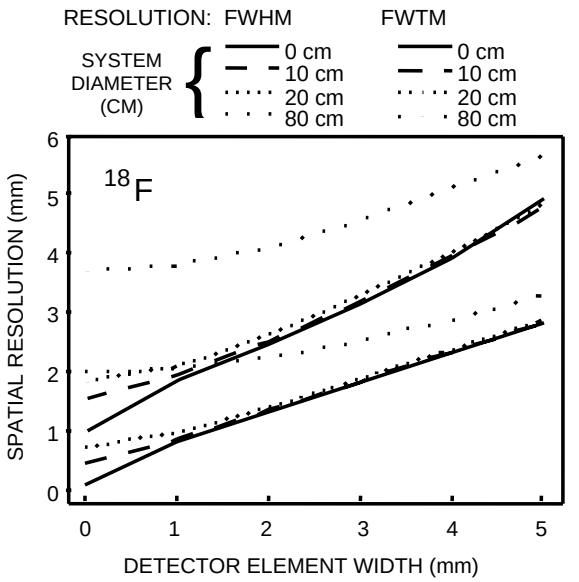

Fig. 12. Calculated ^{18}F PET system spatial resolution limit (FWHM and FWTM) as a function of detector element width for various system diameters (detector separations). For 1 mm detectors and 10 cm detector separation the spatial resolution potential is ~750 μm FWHM. Adapted from Ref. [21].

spatial resolution limits (FWHM and FWTM) for an ^{18}F point source as a function of detector element width for various system detector separations. Again, the detector contribution to the resolution is selectable through a discrete crystal design. With a 1 mm detector element, and a 5–10 cm detector separation, a coincidence imager should be able to attain 750 μm (FWHM) spatial resolution with a sensitivity up to 20 kcps/μCi (50%) for close-proximity imaging. To date, the closest anyone has come to reaching this spatial resolution potential for coincident annihilation photon imaging has been with a gaseous detector system [5], with spatial resolution on the order of 1.5 mm FWHM. However, this system is not optimized for a small FOV, compact breast imager.

5. Summary

We have discussed the importance of the small, dedicated camera concept for functional nuclear emission breast imaging of single-photon and positron emitting tracers from both a performance and practical point of view. One main performance issue is that small FOV, compact imagers can perform close-proximity imaging at multiple orientations to optimize spatial resolution and sensitivity, and reduce background for imaging both types of emissions. We have discussed the particular importance of both spatial and energy resolution for the identification of tiny lesions. Most existing small FOV system scintillation detectors are a result of a compromise between these two performance parameters. We expect that for current small FOV systems, the detectability limits are comparable for both coincident annihilation or single-photon imagers. If available, breast compression decreases photon attenuation and improves spatial resolution, sensitivity, and image contrast. Thus, imaging a compressed breast enhances lesion detectability.

Although there are a few position-sensitive semiconductor detector technologies now available, the most common design used for small FOV breast imagers is a finely segmented inorganic scintillation crystal array coupled to some type of PSPMT. The reasons for this are availability, simplicity, cost and performance related. Particularly appealing for the future is the flat-panel PSPMT because of the combination of high performance and compactness. In the future, when use of semiconductor array devices is more wide spread, and the dream of a $ 1 per pixel array is realized, one may see multiple commercial imaging systems built with photodiodes, avalanche photodiodes, silicon drift detectors, or high band gap compound semiconductors such as CdZnTe.

The selectable spatial resolution available with a finely pixellated detector allows one to push the limits of spatial resolution for emission imaging. For a single detector array, potential spatial resolutions attainable for single- and annihilation photon imaging, due to the intrinsic fundamental physical limitations, are in the neighborhood of 2 mm and 700 μm, respectively, with adequate sensitivity. Of course in order to fully realize this improved spatial resolution potential in the images, it is important to optimize sensitivity enough to maintain adequate S/N per image pixel. Close-proximity imaging allows optimal sensitivity. Such performance improvements available to a dedicated camera may push the breast lesion detectability limits as far as possible.

Acknowledgements

This work was supported in part from grants from the Susan G. Komen Breast Cancer Foundation and the Whitaker Foundation. The author would also like to thank the Instituto Superiore di Sanita' in Rome for the support of this contribution.

References

[1] C.S. Levin, E.J. Hoffman, R.W. Silverman, A.K. Meadors, M.P. Tornai, Breast tumor detectability with small scintillation cameras, Presented at the 1997 IEEE Medical Imaging Conference, Albuquerque, New Mexico.
[2] C.S. Levin, E.J. Hoffman, M.P. Tornai, L.R. MacDonald, IEEE Trans. Nucl. Sci. NS-44(4) (1997) 15130.
[3] S. Majewski, Jefferson National Laboratory, private communication.

[4] F. David Rollo (Ed.), in: Nuclear Medicine Physics, Instrumentation, and Agents, Mosby, 1977.
[5] A.P. Jeavons, R.A. Chandler, C.A.R. Dettmar, IEEE Trans. Nucl. Sci. NS-46(3) (1999) 468.
[6] D. Visvikis, R.J. Ott, K. Wells, M.A. Flower, et al., Nucl. Instr. and Meth. A 392 (1997) 414.
[7] R. Pani, A. Soluri, R. Scafe, A. Pergola, R. Pellegrini, G. De Vincentis, G. Trotta, F. Scopinaro, IEEE Trans. Nucl. Sci. NS-46 (3, part 2) (1999) 702.
[8] S. Majewski, F. Farzanpay, A. Goode, B. Kross, D. Steinbach, A. Weisenberger, M. Williams, R. Wojcik, Nucl. Instr. and Meth. A 409 (1998) 520.
[9] L.R. MacDonald, B.E. Patt, J.S. Ivanczyk, et al., High-resolution hand-held gamma camera. Presented at the 2000 SPIE Medical Applications of Penetrating Radiation Conference, 30 July–4 August, 2000, San Diego, CA.
[10] C.J. Thompson, K. Murthy, Y. Picard, I.N. Weinberg, R. Mako, IEEE Trans. Nucl. Sci. NS-42(4, part 1) (1995) 1012.
[11] G.J. Gruber, W.W. Moses, S.E. Derenzo, IEEE Trans. Nucl. Sci. NS-46(6, part 3) (1999) 2119.
[12] H. Kume, S. Muramatsu, M. Ida, IEEE Trans. Nucl. Sci. NS-33(1) (1986) 359.
[13] R. Wojcik, S. Majewski, D. Steinbach, A.G. Weisenberger, IEEE Trans. Nucl. Sci. NS-45 (3) (1998) 487.
[14] B.E. Patt, J.S. Iwanczyk, C. Rossington Tull, et al., IEEE Trans Nucl Sci. NS-45 (1998) 2126.
[15] Y. Shao, R.W. Silverman, R. Farrell, L. Cirignano, R. Grazioso, K.S. Shah, G. Vissel, M. Clajus, T.O. Tumer, S.R. Cherry, IEEE Trans. Nucl. Sci. NS-47 (3, part 3) (2000) 1051.
[16] C. Fiorini, F. Perotti, C. Labanti, A. Longoni, E. Rossi, Position and energy resolution of a new gamma-ray detector based on a single CsI (Tl) scintillator coupled to a silicon drift chamber array, IEEE Transactions on Nuclear Science, Vol. 46 (4) (1999) 858–864.
[17] Digirad, Inc., San Diego CA.
[18] B.E. Patt, Advance gamma camera detectors, Presented at 1st Topical Symposium on Functional Breast Imaging with Advanced Detectors Rome, April 18–21, 2001.
[19] K.J. Matherson, H.B. Barber, H.H. Barrett, J.D. Eskin, E.L. Dereniak, D.G. Marks, J.M. Woolfenden, E.T. Young, F.L. Augustine, IEEE Trans. Nucl. Sci. NS-45(3) (1998) 354.
[20] J.D. Eskin, H.H. Barrett, H.B. Barber, J. Appl. Phys. 85 (2) (1999) 647.
[21] C.S. Levin, E.J. Hoffman, Phys. Med. Biol. 44 (1999) 781.